AGU ADVANCING EARTH AND SPACE SCIENCES

Geophysical Research Letters

RESEARCH LETTER
10.1029/2025GL119177

Magnetism as a Proxy for Sedimentary REY Enrichment in the Eastern Pacific Ocean and Its Potential Use for Identifying Deep Ocean REY

Yu Fu[1,2], Fei Huang[1], Xiaoming Sun[1,3], Xiaodong Jiang[4], Jieyun Chen[1], Rui Wang[1], Haoyang Zhou[2,5], and Andrew P. Roberts[6]

[1]Guangdong Provincial Key Laboratory of Marine Resources and Coastal Engineering, School of Marine Sciences, Sun Yat-sen University, Zhuhai, China, [2]Guangdong Research Center for Strategic Metals and Green Utilization, Guangzhou, China, [3]School of Earth Sciences and Engineering, Sun Yat-sen University, Zhuhai, China, [4]State Key Laboratory of Marine Resource Utilization in South China Sea, School of Marine Sciences, Hainan University, Haikou, China, [5]Guangzhou Institute of Geochemistry, Chinese Academy of Sciences, Guangzhou, China, [6]Research School of Earth Sciences, Australian National University, Canberra, ACT, Australia

Abstract Rare earth elements and yttrium (REY) are critical for advanced technological and environmental applications. REY-enriched deep-sea sediments have attracted attention as significant potential REY resources. However, efficient identification of these deposits in the open oceans is a persistent challenge. From integrated chemical leaching experiments and geochemical and rock magnetic analyses of two Eastern Pacific Ocean sediment cores, we find a coupled evolution between magnetic signatures and REY concentrations in sediment profiles. Apatite and Fe-Mn (oxy)hydroxides are the primary REY carriers, while biogenic magnetite dominates the magnetic mineral assemblage. We elucidate here mechanistic linkages between mineral magnetic signals and REY enrichment, demonstrating their shared dependence on deep-sea productivity cycles and redox dynamics. We propose that systematic magnetic property analyses could serve as a novel geophysical proxy for identifying REY-rich sediment in marine environments.

Plain Language Summary Rare earth elements and yttrium (REY) are essential for modern technology, from smartphones to renewable energy systems. These valuable elements can be found in deep-sea sediments, but efficient identification of these deposits in the open oceans remains challenging. In this study, we examined sediment samples from the Eastern Pacific Ocean and discovered that magnetite produced by bacteria dominates the magnetic mineral assemblage in REY-enriched sediments, where apatite and Fe-Mn (oxy)hydroxides are the primary REY carriers. Our data suggest that productivity governs formation of both apatite and magnetofossils and drives REY enrichment via liberation of phosphorus, iron, and REY during organic matter remineralization. Coupling of biogenic magnetite and apatite in sediment profiles implies that magnetic properties could be used to identify oceanic REY-rich sediments.

Key Points:

- Biogenic magnetite dominates the magnetic mineral assemblage in Eastern Pacific Ocean rare earth element and yttrium (REY)-enriched sediments
- Oceanic productivity drives REY enrichment and magnetofossil formation
- Magnetic signals have potential for identifying REY-enriched sediments

Supporting Information:

Supporting Information may be found in the online version of this article.

Correspondence to:

X. Sun and X. Jiang,
eessxm@mail.sysu.edu.cn;
jiangxd@hainanu.edu.cn

Citation:

Fu, Y., Huang, F., Sun, X., Jiang, X., Chen, J., Wang, R., et al. (2025). Magnetism as a proxy for sedimentary REY enrichment in the Eastern Pacific Ocean and its potential use for identifying deep Ocean REY. *Geophysical Research Letters*, *52*, e2025GL119177. https://doi.org/10.1029/2025GL119177

Received 3 SEP 2025
Accepted 21 OCT 2025

Author Contributions:

Conceptualization: Yu Fu, Xiaodong Jiang
Data curation: Fei Huang, Rui Wang
Formal analysis: Fei Huang
Funding acquisition: Xiaoming Sun, Haoyang Zhou
Investigation: Yu Fu, Fei Huang, Jieyun Chen
Methodology: Xiaodong Jiang
Supervision: Xiaoming Sun
Writing – original draft: Yu Fu
Writing – review & editing: Xiaodong Jiang, Andrew P. Roberts

1. Introduction

Rare earth element (REE) and yttrium (REY)-enriched deep-sea sediments are distributed widely on the Indian and Pacific Ocean seafloor (Kato et al., 2011; Shi, Bi, et al., 2021). They have attracted global attention due to their significant REY reserves, and could become a strategic alternative to terrestrial REY deposits to meet escalating global demand (Deng et al., 2017; Fujinaga et al., 2016; Iijima et al., 2016; Kim et al., 2022; Menendez et al., 2017). REY-rich sediments are thought to develop mainly in zeolite clay and pelagic clay in deep-sea basins at water depths below the carbonate compensation depth (CCD; Kato et al., 2011; Shi, Bi, et al., 2021). REY are mainly hosted by bioapatite (Kon et al., 2014; Liao, Sun, Li, et al., 2019), and Fe-Mn (hydro)oxides are temporary REY carriers because they scavenge REY from seawater, and are then transformed to bioapatite during early diagenesis (Liao, Sun, Wu, et al., 2019; Takahashi et al., 2015). Many factors such as sedimentation rate, volcanic and hydrothermal activity, redox conditions, primary productivity, and bottom water conditions are considered to be closely related to REY enrichment in deep-sea sediment (Cai et al., 2023; Kato et al., 2011; Ohta et al., 2021; Ren et al., 2021; Resing et al., 2015; Shi, Fu, et al., 2021; F. Wang et al., 2021; Yasukawa et al., 2016). Scientific and technological challenges remain to develop efficient exploration methods to pinpoint REY-rich sediment horizons in deep-sea environments.

Here, we address two questions associated with identifying REY-rich sediment layers. First, are there diagnostic magnetic signatures (e.g., susceptibility anomalies, remanence properties) specific to REY-rich sediments? Second, if the answer to question 1 is yes, what physicochemical mechanisms govern magnetic responses during REY sequestration in authigenic phases? Environmental magnetism can provide records of sediment transportation, deposition, and alteration processes using magnetic techniques (Liu et al., 2012). It can be particularly useful for studying deep-sea sediment below the CCD because the lack of calcareous and siliceous microfossils can hinder the geochemical and paleontological methods generally used in paleoceanographic research (Yamazaki et al., 2020), and can provide an archive of oceanic paleoenvironmental information (Chang et al., 2018; Hesse, 1994; Kopp & Kirschvink, 2008; Roberts et al., 2011; Yamazaki, 2012). To explore relationships between mineral magnetism and sedimentary REY-enrichment, chemical leaching, geochemical, and magnetic analyses were conducted on two Eastern Pacific Ocean sediment cores with high REY contents. We use a multidisciplinary approach to investigate the environmental processes governing REY enrichment in these deep-sea sediments.

2. Materials and Methods

Site U1334 (7°59.998′N, 131°58.408′W) is situated at water depths of 5,000–5,100 m, ∼100 km north of the Clipperton Fracture Zone on abyssal hill topography (Figure 1). Site 319 (13°01.04′S, 101°31.46′W) is positioned in the abyssal southeast Pacific Ocean at 4,290 m water depth, and lies 1,100 km east of the East Pacific Rise (EPR) and 600 km west of the dormant Galapagos Rise spreading center (Dymond et al., 1977; Figure 1). Details of samples and their geological background are described in Appendix S1 in Supporting Information S1.

2.1. Mineralogical and Bulk Elemental Measurements

Mineral identification from four powdered samples was performed using a Rigaku Rapid II X-ray diffraction instrument (Mo Kα radiation) at the School of Marine Sciences, Sun Yat-sen University (SYSU). Microstructural observation of minerals in the sediment was performed at SYSU, with a TESCAN MIRA Field Emission scanning electron microscope coupled with a Bruker XFlash 6160 Energy Dispersive Spectrometer. Bulk-sediment elemental analyses were performed by inductively coupled plasma-optical emission spectroscopy (ICP-OES) and inductively coupled plasma-mass spectrometry (ICP-MS) at the ALS Chemex laboratory.

2.2. Sequential Chemical Extraction

Chemical leaching was employed to assess quantitatively specific contributions of different mineral components in bulk sediments to the total REY content (Kim et al., 2022; Liao et al., 2022; Paul et al., 2019). Initial stages of chemical leaching experiments were conducted in an ultra-clean laboratory at 20°C. In each leaching scheme, ∼200 mg of finely ground sample was sieved to 200 mesh and placed into a 50 ml centrifuge tube reaction vessel, with a nominal volume of 25 ml of leaching solution added at each step. During leaching, centrifuge tubes containing the sample-leachate mixture were placed on a shaker to ensure constant solid particle suspension, allowing maximum contact area with the leachate and subsequent reaction. The following leaching procedures were used to separate REE reservoirs into 6 fractions.

1. Calcium carbonate and calcium phosphate were removed by adding 25 ml of 1 M acetic acid/Na-acetate buffer at pH 4.5, shaking for 24 hr, followed by centrifugation at 4,000 rpm for 10 min to separate the supernatant, and filtering through a 0.2 μm membrane filter to extract the leachate. Residual solids were washed with ultrapure water for 2 hr, followed by repeated centrifugation and filtration steps for extraction.
2. Easily reducible manganese and iron-oxides were removed by suspended leaching in 25 ml of 0.1 M hydroxylamine-HCl at pH 2 for 2 hr. Extraction of leachate and washing steps are the same as above.
3. Moderately reducible iron-oxides were removed by suspended leaching in 25 ml of 0.1 M hydroxylamine-HCl at pH 2 for 48 hr. Extraction of leachate and washing steps are as above.
4. Reducible iron-oxides were removed by suspended leaching in 25 ml of Na-dithionite (50 g/l)/0.2 M Na-citrate solution at pH 4.8 for 2 hr. Extraction of leachate and washing steps are as above.
5. Magnetite was removed by suspended leaching in 25 ml of 0.2 M NH_4-oxalate/0.17 M oxalic acid at pH 3.5 for 6 hr. Extraction of leachate and washing steps are as above.

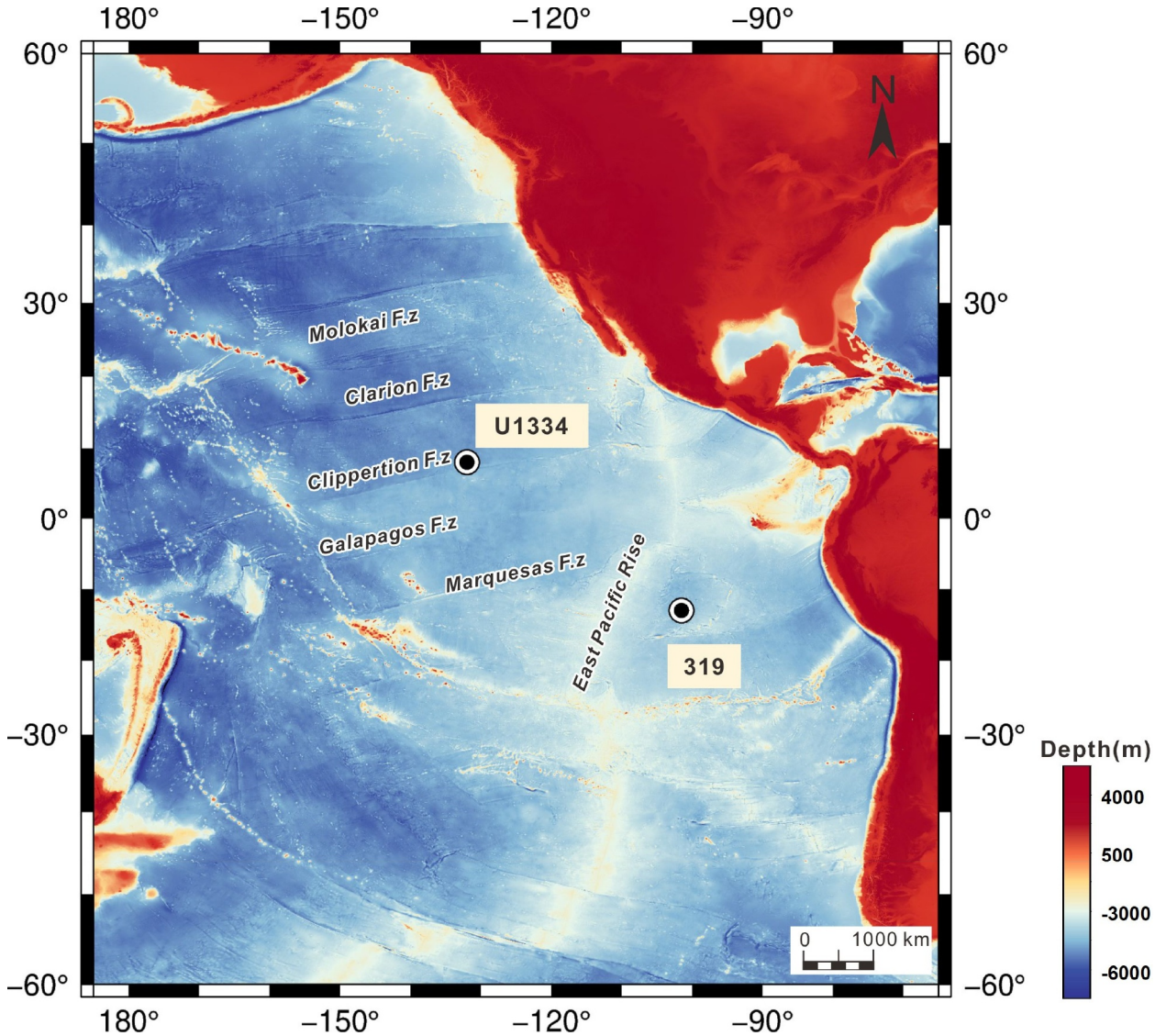

Figure 1. Locations of the two studied sites in the Eastern Pacific Ocean.

6. The residue (mainly composed of aluminosilicate and biogenic silica) was dried and weighed for each sample to calculate the mass percentage of each phase. Subsequently, similar to the method for bulk-sediment rare earth elements, REE contents were determined using fusion ICP-MS.

After completing the leaching experiments, REE concentrations in the leachates were measured using ICP-MS at the Laboratory of Marine Resources and Coastal Engineering, Guangdong Province, with an Agilent 7700x ICP-MS equipped with an Agilent ASX-5000 autosampler. The relative standard deviation was commonly below 3% of the detected elements.

2.3. Magnetic Measurements and Microscopic Observation

Magnetic measurements were made at the School of Earth Science and Engineering, SYSU. The magnetic susceptibility (χ) was measured at room temperature at 976 and 15,767 Hz, respectively, using a Kappabridge susceptometer (MFK2-FA). The frequency dependence of susceptibility ($(\chi_{fd} = \chi_{976Hz} - \chi_{15,676Hz})/\chi_{976Hz}$) was obtained, which is sensitive to superparamagnetic (SP) particles (Liu et al., 2005). An anhysteretic remanent magnetization (ARM) was imparted in an alternating field demagnetizer (D-Tech 2000) by subjecting samples to an alternating magnetic field decaying from a 100 mT peak field, at 50 μT per half cycle, superimposed on a direct

current field of 0.05 mT. The remanence was then measured using a JR-6A spinner magnetometer. The susceptibility of ARM (χ_{ARM}) was calculated by normalizing the ARM by the direct field. A saturation isothermal remanent magnetization (SIRM) was imparted to the sample in a 1 T direct field. Then, a field of 0.3 T was applied in the opposite direction to the SIRM to obtain information about the low coercivity, ferrimagnetic fraction ($IRM_{-0.3T}$). 'Hard' isothermal remanent magnetization (HIRM) values were calculated using ($IRM_{-0.3T}$ + SIRM)/2. A vibrating sample magnetometer (VSM 3900) was used to measure first-order reversal curves (FORCs; Pike et al., 1999) and IRM acquisition curves. The measured FORC data were processed using the FORCinel v3.06 software, with a smoothing factor of 3 (Harrison & Feinberg, 2008).

Representative samples were selected for magnetic mineral extraction and were analyzed using a transmission electron microscope (TEM). TEM observations were made with a FEI Talos F200S at 200 kV at the Guangzhou Institute of Geochemistry, Chinese Academy of Sciences.

3. Results

3.1. Mineralogy and Geochemistry of Bulk Sediments

Most of the studied sediments consist of phillipsite, smectite, calcite, apatite (including fish teeth), quartz, and iron-manganese (hydro)oxides (Figure S1 in Supporting Information S1). The calcite contents of REY-enriched layers is relatively low (<1.5%), with clay components predominating, while REY-depleted layers have higher calcite contents (Figure S1a in Supporting Information S1).

Elemental compositions (Table S1, https://doi.org/10.5281/zenodo.17336447) reveal distinct geochemical patterns between the two cores. Calcium has large variations in both U1334 (1.0%–33.7%) and 319 (2.1%–34.8%), while P and Fe have depth-dependent trends: their concentrations decline with depth in U1334, whereas elevated P and Fe are maintained in shallow layers of core 319, with maximum values of 0.7% and 14.0%, respectively. Biogenic barium (Ba_{bio}) is associated with sinking organic matter (Dymond et al., 1992; Schoepfer et al., 2015), which is calculated as follows (Dymond et al., 1992):

$$Ba_{bio} = Ba_{total} - Al \times (Ba/Al)_{detr},$$

where $(Ba/Al)_{detr}$ denotes the Ba content from detrital phases. The influence of detrital Ba on Ba_{bio} is relatively minor in the abyssal ocean; biogenic barium makes up >90% of the total Ba in all samples (Table S1, https://doi.org/10.5281/zenodo.17336447). REY contents vary greatly in the two studied cores. All samples have flat Post-Archean Australian Shale (PAAS)-normalized REY patterns with marked negative Ce anomalies (δCe = 0.13–0.45; average: 0.22) (Figures S2a and S2b in Supporting Information S1). Ce anomalies are used widely to trace paleoceanographic redox conditions (e.g., Tostevin et al., 2016; Y. L. Wang et al., 1986). Generally, under oxic conditions, Ce^{3+} oxidizes to insoluble Ce^{4+} and is incorporated into sedimentary Mn oxides (Goldberg et al., 1963; Piper, 1974), which increases δCe values in clay sediments.

3.2. Sequential Leaching Results

The REY proportion leached out in "step one" was highest for all steps in U1334 (excluding Ce) (Table S2, https://doi.org/10.5281/zenodo.17336447), and accounts for up to 88.1% of the total sediment (Figure S2c in Supporting Information S1). Rare earth partitioning curves for "step one" for all samples have a left-leaning trend and significant negative Ce anomalies, with positive Y anomalies at Site 319 (Figure S2d in Supporting Information S1). Unlike U1334, most REY in samples from Site 319 are leached out in "step two" and "step three," with total proportions of 43.4%–52.8% (Table S2, https://doi.org/10.5281/zenodo.17336447). For U1334, 8.4%–22.4%, and 12.5%–22.2% of REY is leached in the second and third steps, respectively. Rare earth partitioning patterns for leachates in "step two" and "step three" have noticeable positive Eu anomalies and less obvious Ce anomalies than "step one", with negative Y anomalies at Site 319 (Figures S2e and S2f in Supporting Information S1). Only 1.0%–1.4% and 8.7%–17.1% of REY were leached out in "step four" for U1334 and 319, and mostly less than 3% in "step five." Due to uncertainties in the experimental procedure and analytical errors, the ΣREY recovery rate of samples ranges from 82% to 121%, with most falling between 90% and 100%.

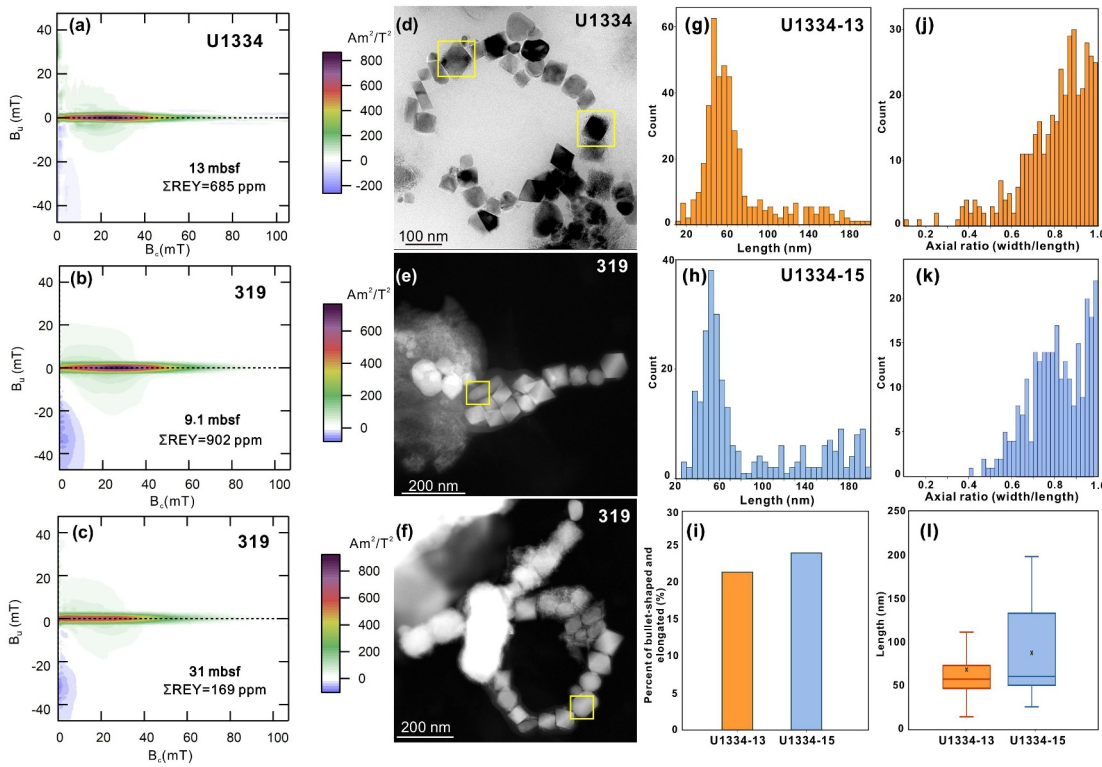

Figure 2. FORC diagrams (a–c), transmission electron microscope images of magnetofossil chains (d–f), and conventional magnetofossil morphological data (g–l) for representative samples from Site U1334 and core 319. Morphological data include histograms of magnetofossil length (g, h) and axial ratio (j, k), percentage of bullet-shaped and elongated magnetofossils (i), and magnetofossil length box charts (l) for Site U1334. All FORC diagrams have contours distributed predominantly along the horizontal axis ($B_u = 0$), which indicates the presence of magnetostatically non-interacting stable single-domain particles. High-resolution-TEM images with Fourier transform patterns for the magnetofossils indicated in yellow boxes (d–f) are shown in Figure S5 in Supporting Information S1. The upper and lower box boundaries in (l) represent the third (Q3) and first quartiles (Q1), respectively. The top and bottom whiskers represent Q3 + 1.5 × (Q3 − Q1) and Q1 − 1.5 × (Q3 − Q1), respectively. The horizontal line and cross marks inside the boxes represent the median and mean, respectively. The names 1334-13 and 1334-15 denote samples at depths of 13 and 15 mbsf, respectively.

3.3. Magnetic Properties and Morphological Features of Magnetofossils

From Figure S3 in Supporting Information S1 and Table S3, https://doi.org/10.5281/zenodo.17336447, χ, χ_{ARM}, SIRM, $IRM_{-300\ mT}$, and HIRM variation patterns for the Site U1334 and core 319 sediments are similar to REY variations, with a stepwise increase with depth from bottom to top (Figure S3 in Supporting Information S1). Both cores have consistently high χ, which indicates ferrimagnetic mineral dominance (Liu et al., 2012). χ_{ARM} can be used to indicate the relative abundance of the stable single-domain (SD) fraction (Roberts et al., 2012; Zhang et al., 2022). With few exceptions, χ_{ARM}/SIRM has little variation, which suggests a predominance of SD magnetic particles and that magnetic mineral grain size remains relatively consistent from top to bottom. FORC diagrams (Pike et al., 1999; Roberts et al., 2000) for sediments from sites U1334 and 319 have a central ridge along the B_c axis (Figure 2a–2c), which indicates negligible magnetostatic interactions and potentially the presence of intact magnetofossil chains (Chang et al., 2014; Chen et al., 2007; Egli et al., 2010; Roberts et al., 2012). Unmixing of IRM acquisition curve analyses also confirm the dominant magnetofossil contribution (Figure S4 in Supporting Information S1).

TEM observations of magnetic particles from representative samples from the two cores confirm the presence of abundant conventional magnetofossils (Figure 2d–2f). All of the magnetofossils have morphologies and crystal structures similar to typical magnetosomal crystals (Bazylinski & Frankel, 2004; Kopp & Kirschvink, 2008). From electron diffraction patterns (Figure S5 in Supporting Information S1), the primary magnetofossil phases are identified as magnetite. The magnetofossils are classified into three groups according to shape: bullet-shaped, elongated, and equant (Chang et al., 2018; Yamazaki et al., 2019). As shown in Figure 2g–2l, the abundance of

bullet-shaped and elongated magnetofossils in sample U1334-13 is lower than in sample U1334-15 (Figure 2i). Magnetofossils in sample U1334-15 are generally larger than in sample U1334-13 (Figure 2l).

4. Discussion

4.1. REY Carrier Minerals

Leaching experiments for Site U1334 indicate that the primary REY carrier is Ca-phosphate with negligible contributions from Ca-carbonate because carbonate is generally REY-depleted (generally <10 ppm). Fossil bioapatite and authigenic apatite have considerable ΣREY contents in REY-enriched deep-sea sediment (Hong et al., 2024; Kashiwabara et al., 2018; Kon et al., 2014), so apatite is thought to be an important REY carrier (Kashiwabara et al., 2014; Liao et al., 2022). Our results indicate that REY in "step one" leachates have characteristics consistent with those of apatite from REY-rich deep-sea mud. Therefore, Ca-phosphate (including bioapatite) is the main REY carrier mineral at Site U1334, with ΣREY contents controlled by the apatite content, which is supported by coordinated variations between P and ΣREY (Figure 3a). Fe-Mn phases are the dominant REY carriers in core 319, which is located near the EPR where volcanic-hydrothermal activity delivers significant Fe and Mn contents. Elevated Fe and Mn concentrations and covariation between Fe/Mn and REY contents (Figures 3f and 3h) further supports this hypothesis. Overall, the primary REY host in REY-enriched sediments may vary between apatite and Fe-Mn (hydro)oxides, depending on the region sampled.

4.2. REY Enrichment Mechanism of Eastern Pacific Ocean Deep-Sea Sediment

Most samples from Sites U1334 and 319 have co-varying ΣREY and Ba_{bio} contents (Figures 3b and 3g). Enhanced biological productivity increases the organic matter content, which facilitates REY enrichment in deep-sea sediment by supplying a REY source (Figure 4) via scavenging and remineralization within the water column (Freslon et al., 2014; Pavlova et al., 2023). Increased productivity can also elevate seawater phosphorus, thereby promoting apatite formation (Ohta et al., 2020), which can adsorb abundant REY (Kon et al., 2014; Liao et al., 2022; Takaya et al., 2018), as indicated by leaching results for U1334. Despite the predominance of REY within Fe-Mn (hydro)oxides in core 319, P contents in REY-enriched layers exceed significantly those of Site U1334 (Figures 3b and 3g). This suggests that high productivity governs REY enrichment in core 319, whereas dominance of Fe-Mn phases as the primary REY hosts at Site 319 arises from its proximity to the EPR. EPR hydrothermal activity supplies elevated Fe contents to seawater (Resing et al., 2015; Tagliabue et al., 2010), which serves as a potential nutrient source to the surface ocean, triggering episodic productivity enhancement (Ardyna et al., 2019; Schine et al., 2021). The high EPR supply of Fe and Mn (Figure 3h), thus, drives Fe-Mn (hydro)oxide formation; these phases have high surface area and can adsorb large REY contents (Ren et al., 2024; Zhou et al., 2020) to facilitate sediment REY enrichment.

Consistent variations between ΣREY contents and δCe values of bulk sediment for most samples suggests a relatively oxygenated environment during REY enrichment (Figures 3d and 3i), although Ce behavior in seawater is not only controlled by redox, but also by factors such as pH, P concentration, terrigenous input, and diagenetic conditions (Cao et al., 2022; MacLeod & Irving, 1996; Pattan et al., 2005). Magnetofossil morphology is used widely to estimate deep-ocean redox conditions. The relative abundance of magnetofossils with equant octahedral morphology increases in more oxic environments, while elongated and bullet-shaped forms are produced at lower oxygen contents (Chang et al., 2018; Hesse, 1994; Katzmann et al., 2013; Li & Pan, 2012; Yamazaki & Ikehara, 2012; Yamazaki et al., 2019). From the magnetofossil assemblages, the average size and elongation of magnetosomal crystals decrease from lower to upper layers (Figure 2g–2l), which reflects an increase in deep-sea oxygenation. Oxic seawater enables precipitation of colloids of hydrated Mn and Fe oxides, which acquire trace metals by surface sorption (Glasby, 2006; Hein et al., 2013). These processes are important for REY enrichment in deep-sea sediment because Fe-Mn (hydro)oxides act as the primary REY host in sediments, and as a temporary REY host, which can be dissolved and then sequestered in phosphate minerals (e.g., bioapatite) during early diagenesis (Liao, Sun, Wu, et al., 2019; Takahashi et al., 2015). Also, REY can be sourced from organic matter degradation in oxic seawater (Grybos et al., 2007; Haley et al., 2004), bottom waters, and sediment pore waters to contribute to REY enrichment in deep-sea mud (Figure 4).

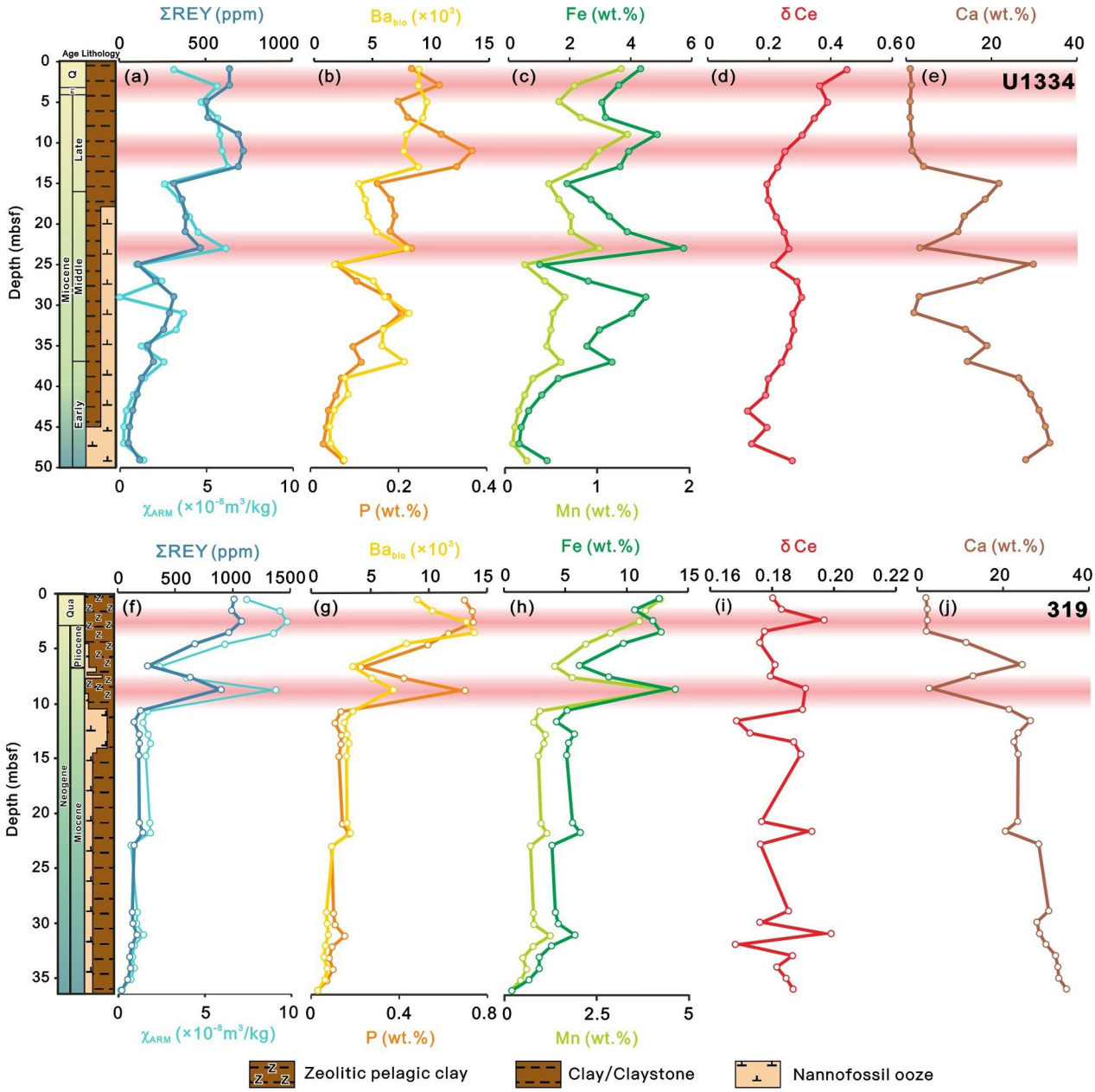

Figure 3. Comparison of ΣREY contents, geochemical characteristics, and magnetic properties from Site U1334 (a–e) and core 319 (f–j). Note that for Site U1334 and core 319, ΣREY, Fe, Mn, P, χ_{ARM}, and Ba_{bio} values co-vary. Core 319 has higher Fe, Mn, and P concentrations than Site U1334. Red bars indicate REY-enriched layers.

4.3. Mineral Magnetic Co-Variation With Sedimentary REY Enrichment

As shown in Figure S3 in Supporting Information S1, relevant magnetic parameters covary with ΣREY contents throughout the cores, which suggests that the environment that produces the dominant magnetic particles also meets the conditions required for REY enrichment. Magnetofossils are the main magnetic component at sites U1334 and 319 as evidenced by FORC, IRM, and TEM data, with χ_{ARM} representing their abundance. Although SP particles are also evidently present, as indicated by χ_{fd} (Figure S3 in Supporting Information S1), their variations are not consistent with those of other magnetic parameters and of REY variations, so we do not discuss their variations further. Sedimentary magnetofossil concentration depends mainly on the interplay of magnetosome production and dissolution. Magnetofossil dissolution can be excluded here because of the relatively oxic conditions, as indicated by δCe and magnetofossil morphology (Kodama et al., 2013; Liu et al., 2015). Thus,

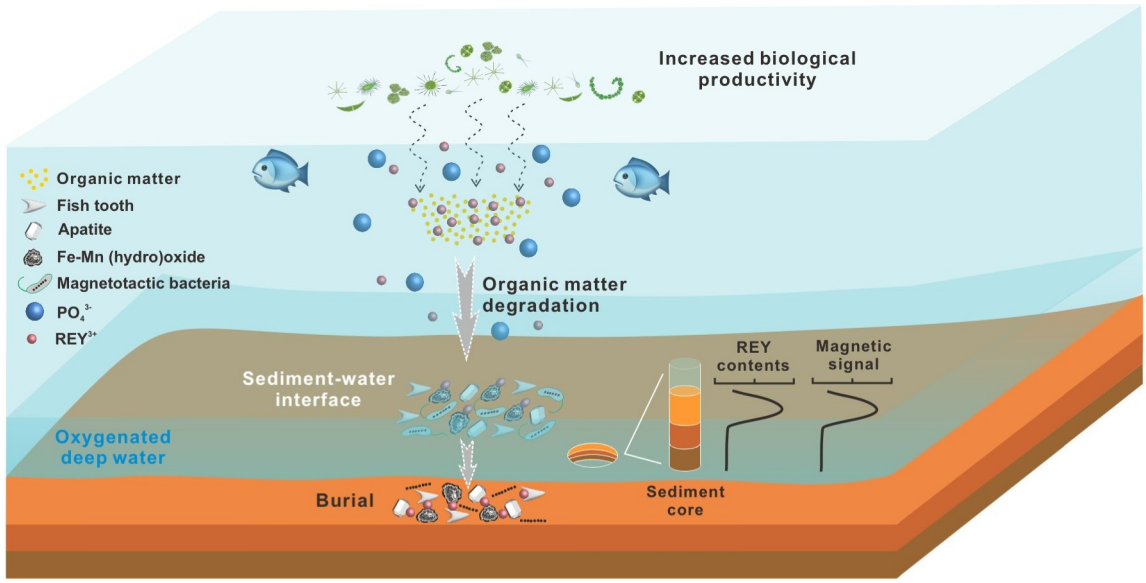

Figure 4. Schematic model of rare earth element and yttrium (REY) enrichment and associated magnetic response in Eastern Pacific Ocean sediments. Depth profiles on the bottom right illustrate how REY contents and magnetism vary in the sediment, which are analyzed based on discrete sediment core samples.

consistent ΣREY and χ_{ARM} variations (Figures 3a and 3f) suggest that REY concentrations have high correlation with magnetosome production. Increased nutrient supply can boost bacterial magnetite abundance via export of particulate iron and organic carbon to the seafloor (Larrasoaña et al., 2012; Roberts et al., 2011; Yamazaki & Horiuchi, 2016; Zhang et al., 2021). Although Fe-Mn phases are the primary REY hosts in core 319, the REY source is from organic matter degradation linked to productivity. Therefore, REY and magnetofossil contents are both controlled by nutrient supply and organic matter degradation governed by productivity, which produces the covariation between REY and magnetic contents (Figure S6 in Supporting Information S1). If productivity is high, delivery of elevated organic matter contents to the seafloor can produce anoxic sulfidic conditions that cause magnetofossils to dissolve (e.g., Roberts, 2015). Positive correlation between productivity and magnetofossil content is most likely in high nitrate-low chlorophyll oceans where iron limitation constrains productivity. Delivery of biologically available iron to surface waters via atmospheric dust or hydrothermal plumes can fertilize productivity episodes that delivers organic matter to the seafloor to produce iron-reducing, but not sulfate reducing, early diagenetic sedimentary conditions that enhance magnetotactic bacteria abundance (Roberts et al., 2011) to produce a correlation between magnetofossil and REY contents.

Although REY enriched mineral contents vary in Eastern Pacific Ocean sediments, REY contents are coupled tightly to biogenic magnetite variations, which are governed by productivity and deep-ocean redox conditions. Therefore, sedimentary magnetic signals have great potential for identifying REY-enriched east Pacific basin sediments, particularly in iron-limited parts of the global ocean.

5. Conclusions

We find that Ca-phosphate and Fe-Mn (hydro)oxides are the two main REY carrier mineral types in the Eastern Pacific Ocean based on magnetic and geochemical analyses of two sediment cores. Our results indicate that productivity drives REY enrichment and magnetofossil formation through release of substantial P, Fe, and REY during organic matter degradation, while oxic seafloor conditions facilitate further organic matter degradation and Fe-Mn (hydro)oxide formation. This covariation mechanism for REY contents and biogenic magnetite variations in our study provides a solid foundation for exploration of REY-enriched deep-sea sediments.

Conflict of Interest

The authors declare no conflicts of interest relevant to this study.

Data Availability Statement

Data is available at Fu (2025).

Acknowledgments
Funding for this research was provided by the National Natural Science Foundation of China (42572072, 92262304, and 42476049) and the Open Fund of the Guangdong Research Center for Strategic Metals and Green Utilization (Supported by Guangdong S&T Program 2024B0303390002). Samples were provided by the International Ocean Discovery Program (IODP). The authors thank Xiaoqiang Yang for assistance with magnetic analyses. We also thank Ioan Lascu for his helpful comments that improved the paper.

References

Ardyna, M., Lacour, L., Sergi, S., d'Ovidio, F., Sallée, J.-B., Rembauville, M., et al. (2019). Hydrothermal vents trigger massive phytoplankton blooms in the Southern Ocean. *Nature Communications*, *10*(1), 2451. https://doi.org/10.1038/s41467-019-09973-6

Bazylinski, D. A., & Frankel, R. B. (2004). Magnetosome formation in prokaryotes. *Nature Reviews Microbiology*, *2*(3), 217–230. https://doi.org/10.1038/nrmicro842

Cai, Y.-C., Shi, X., Zhou, T., Huang, M., Yu, M., Zhang, Y., et al. (2023). Evaluating the contribution of hydrothermal fluids and clay minerals to the enrichment of rare earth elements and yttrium (REY) in deep-sea sediments. *Ore Geology Reviews*, *161*, 105679. https://doi.org/10.1016/j.oregeorev.2023.105679

Cao, C., Liu, X.-M., & Chen, J. (2022). Cerium anomaly as a tracer for paleo-oceanic redox conditions: A thermodynamics-based Ce oxidation modeling approach. *Frontiers in Earth Science*, *10*, 927826. https://doi.org/10.3389/feart.2022.927826

Chang, L., Harrison, R. J., Zeng, F., Berndt, T. A., Roberts, A. P., Heslop, D., & Zhao, X. (2018). Coupled microbial bloom and oxygenation decline recorded by magnetofossils during the Palaeocene–Eocene Thermal Maximum. *Nature Communications*, *9*(1), 4007. https://doi.org/10.1038/s41467-018-06472-y

Chang, L., Roberts, A. P., Winklhofer, M., Heslop, D., Dekkers, M. J., Krijgsman, W., et al. (2014). Magnetic detection and characterization of biogenic magnetic minerals: A comparison of ferromagnetic resonance and first-order reversal curve diagrams. *Journal of Geophysical Research*, *119*(8), 6136–6158. https://doi.org/10.1002/2014jb011213

Chen, A. P., Egli, R., & Moskowitz, B. M. (2007). First-order reversal curve (FORC) diagrams of natural and cultured biogenic magnetic particles. *Journal of Geophysical Research*, *112*(B8). https://doi.org/10.1029/2006jb004575

Deng, Y., Ren, J., Guo, Q., Cao, J., Wang, H., & Liu, C. (2017). Rare earth element geochemistry characteristics of seawater and porewater from deep sea in western Pacific. *Scientific Reports*, *7*(1), 16539. https://doi.org/10.1038/s41598-017-16379-1

Dymond, J., Corliss, J. B., & Heath, G. R. (1977). History of metalliferous sedimentation at deep sea drilling site 319 in the South Eastern Pacific. *Geochimica et Cosmochimica Acta*, *41*(6), 741–753. https://doi.org/10.1016/0016-7037(77)90045-X

Dymond, J., Suess, E., & Lyle, M. (1992). Barium in deep-sea sediment: A geochemical proxy for paleoproductivity. *Paleoceanography*, *7*(2), 163–181. https://doi.org/10.1029/92PA00181

Egli, R., Chen, A. P., Winklhofer, M., Kodama, K. P., & Horng, C.-S. (2010). Detection of noninteracting single domain particles using first-order reversal curve diagrams. *Geochemistry, Geophysics, Geosystems*, *11*(1). https://doi.org/10.1029/2009gc002916

Freslon, N., Bayon, G., Toucanne, S., Bermell, S., Bollinger, C., Cheron, S., et al. (2014). Rare earth elements and neodymium isotopes in sedimentary organic matter. *Geochimica et Cosmochimica Acta*, *140*, 177–198. https://doi.org/10.1016/j.gca.2014.05.016

Fu, Y. (2025). Magnetism as a proxy for sedimentary REY enrichment in the Eastern Pacific Ocean and its potential use for identifying deep Ocean REY [Dataset]. *Zenodo*. https://doi.org/10.5281/zenodo.17336447

Fujinaga, K., Yasukawa, K., Nakamura, K., Machida, S., Takaya, Y., Ohta, J., et al. (2016). Geochemistry of REY-rich mud in the Japanese Exclusive Economic Zone around Minamitorishima Island. *Geochemical Journal*, *50*(6), 575–590. https://doi.org/10.2343/geochemj.2.0432

Glasby, G. P. (2006). Manganese: Predominant role of nodules and crusts. In *Marine geochemistry* (pp. 371–427). Springer.

Goldberg, E. D., Koide, M., Schmitt, R. A., & Smith, R. H. (1963). Rare-Earth distributions in the marine environment. *Journal of Geophysical Research*, *68*(14), 4209–4217. https://doi.org/10.1029/JZ068i014p04209

Grybos, M., Davranche, M., Gruau, G., & Petitjean, P. (2007). Is trace metal release in wetland soils controlled by organic matter mobility or Fe-oxyhydroxides reduction? *Journal of Colloid and Interface Science*, *314*(2), 490–501. https://doi.org/10.1016/j.jcis.2007.04.062

Haley, B. A., Klinkhammer, G. P., & McManus, J. (2004). Rare earth elements in pore waters of marine sediments. *Geochimica et Cosmochimica Acta*, *68*(6), 1265–1279. https://doi.org/10.1016/j.gca.2003.09.012

Harrison, R. J., & Feinberg, J. M. (2008). FORCinel: An improved algorithm for calculating first-order reversal curve distributions using locally weighted regression smoothing. *Geochemistry, Geophysics, Geosystems*, *9*(5), 2008GC001987. https://doi.org/10.1029/2008GC001987

Hein, J. R., Mizell, K., Koschinsky, A., & Conrad, T. A. (2013). Deep-ocean mineral deposits as a source of critical metals for high- and green-technology applications: Comparison with land-based resources. *Ore Geology Reviews*, *51*, 1–14. https://doi.org/10.1016/j.oregeorev.2012.12.001

Hesse, P. P. (1994). Evidence for bacterial palaeoecological origin of mineral magnetic cycles in oxic and sub-oxic Tasman Sea sediments. *Marine Geology*, *117*(1–4), 1–17. https://doi.org/10.1016/0025-3227(94)90003-5

Hong, S. K., Kim, Y., & Kim, Y.-M. (2024). Assessment of REY resource potential in deep-sea sediments with Fe–Mn (oxyhydr)oxides in the Pacific Ocean. *Journal of Geochemical Exploration*, *267*, 107581. https://doi.org/10.1016/j.gexplo.2024.107581

Iijima, K., Yasukawa, K., Fujinaga, K., Nakamura, K., Machida, S., Takaya, Y., et al. (2016). Discovery of extremely REY-rich mud in the western North Pacific Ocean. *Geochemical Journal*, *50*(6), 557–573. https://doi.org/10.2343/geochemj.2.0431

Kashiwabara, T., Toda, R., Fujinaga, K., Honma, T., Takahashi, Y., & Kato, Y. (2014). Determination of host phase of lanthanum in deep-sea REY-rich mud by XAFS and μ-XRF using high-energy synchrotron radiation. *Chemistry Letters*, *43*(2), 199–200. https://doi.org/10.1246/cl.130853

Kashiwabara, T., Toda, R., Nakamura, K., Yasukawa, K., Fujinaga, K., Kubo, S., et al. (2018). Synchrotron X-ray spectroscopic perspective on the formation mechanism of REY-rich muds in the Pacific Ocean. *Geochimica et Cosmochimica Acta*, *240*, 274–292. https://doi.org/10.1016/j.gca.2018.08.013

Kato, Y., Fujinaga, K., Nakamura, K., Takaya, Y., Kitamura, K., Ohta, J., et al. (2011). Deep-sea mud in the Pacific Ocean as a potential resource for rare-earth elements. *Nature Geoscience*, *4*(8), 535–539. https://doi.org/10.1038/ngeo1185

Katzmann, E., Eibauer, M., Lin, W., Pan, Y., Plitzko, J. M., & Schüler, D. (2013). Analysis of magnetosome chains in magnetotactic bacteria by magnetic measurements and automated image analysis of electron micrographs. *Applied and Environmental Microbiology*, *79*(24), 7755–7762. https://doi.org/10.1128/AEM.02143-13

Kim, M. G., Hyeong, K., & Yoo, C. M. (2022). Distribution of rare Earth elements and yttrium in sediments from the Clarion-Clipperton Fracture Zone, Northeastern Pacific Ocean. *Geochemistry, Geophysics, Geosystems*, *23*(7), 1–13. https://doi.org/10.1029/2022GC010454

Kodama, K. P., Moeller, R. E., Bazylinski, D. A., Kopp, R. E., & Chen, A. P. (2013). The mineral magnetic record of magnetofossils in recent lake sediments of Lake Ely, PA. *Global and Planetary Change*, *110*, 350–363. https://doi.org/10.1016/j.gloplacha.2013.03.012

Kon, Y., Hoshino, M., Sanematsu, K., Morita, S., Tsunematsu, M., Okamoto, N., et al. (2014). Geochemical characteristics of apatite in heavy REE-rich deep-sea mud from Minami-Torishima Area, Southeastern Japan: Apatite in heavy REE-rich deep-sea mud. *Resource Geology*, *64*(1), 47–57. https://doi.org/10.1111/rge.12026

Kopp, R. E., & Kirschvink, J. L. (2008). The identification and biogeochemical interpretation of fossil magnetotactic bacteria. *Earth-Science Reviews*, *86*(1–4), 42–61. https://doi.org/10.1016/j.earscirev.2007.08.001

Larrasoaña, J. C., Roberts, A. P., Chang, L., Schellenberg, S. A., Fitz Gerald, J. D., Norris, R. D., & Zachos, J. C. (2012). Magnetotactic bacterial response to Antarctic dust supply during the Palaeocene–Eocene thermal maximum. *Earth and Planetary Science Letters*, *333–334*, 122–133. https://doi.org/10.1016/j.epsl.2012.04.003

Li, J., & Pan, Y. (2012). Environmental factors affect magnetite magnetosome synthesis in *Magnetospirillum magneticum* AMB-1: Implications for biologically controlled mineralization. *Geomicrobiology Journal*, *29*(4), 362–373. https://doi.org/10.1080/01490451.2011.565401

Liao, J., Chen, J., Sun, X., Wu, Z., Deng, Y., Shi, X., et al. (2022). Quantifying the controlling mineral phases of rare-earth elements in deep-sea pelagic sediments. *Chemical Geology*, *595*, 120792. https://doi.org/10.1016/j.chemgeo.2022.120792

Liao, J., Sun, X., Li, D., Sa, R., Lu, Y., Lin, Z., et al. (2019). New insights into nanostructure and geochemistry of bioapatite in REE-rich deep-sea sediments: LA-ICP-MS, TEM, and Z-contrast imaging studies. *Chemical Geology*, *512*, 58–68. https://doi.org/10.1016/j.chemgeo.2019.02.039

Liao, J., Sun, X., Wu, Z., Sa, R., Guan, Y., Lu, Y., et al. (2019). Fe-Mn (oxyhydr)oxides as an indicator of REY enrichment in deep-sea sediments from the central North Pacific. *Ore Geology Reviews*, *112*, 103044. https://doi.org/10.1016/j.oregeorev.2019.103044

Liu, Q., Roberts, A. P., Larrasoaña, J. C., Banerjee, S. K., Guyodo, Y., Tauxe, L., & Oldfield, F. (2012). Environmental magnetism: Principles and applications. *Reviews of Geophysics*, *50*, RG4002. https://doi.org/10.1029/2012RG000393

Liu, Q., Yu, Y., Pan, Y., Zhu, R., & Zhao, X. (2005). Partial anhysteretic remanent magnetization (pARM) of synthetic single- and multidomain magnetites and its paleoenvironmental significance. *Chinese Science Bulletin*, *50*(20), 2381–2384. https://doi.org/10.1360/982005-178

Liu, S., Deng, C., Xiao, J., Li, J., Paterson, G. A., Chang, L., et al. (2015). Insolation driven biomagnetic response to the Holocene Warm Period in semi-arid East Asia. *Scientific Reports*, *5*(1), 8001. https://doi.org/10.1038/srep08001

MacLeod, K. G., & Irving, A. J. (1996). Correlation of cerium anomalies with indicators of paleoenvironment. *Journal of Sedimentary Research*, *66*(5), 948–955. https://doi.org/10.1306/d426844b-2b26-11d7-8648000102c1865d

Menendez, A., James, R. H., Roberts, S., Peel, K., & Connelly, D. (2017). Controls on the distribution of rare earth elements in deep-sea sediments in the North Atlantic Ocean. *Ore Geology Reviews*, *87*, 100–113. https://doi.org/10.1016/j.oregeorev.2016.09.036

Ohta, J., Yasukawa, K., Nakamura, K., Fujinaga, K., Iijima, K., & Kato, Y. (2021). Geological features and resource potential of deep-sea mud highly enriched in rare-earth elements in the Central Pacific Basin and the Penrhyn Basin. *Ore Geology Reviews*, *139*, 104440. https://doi.org/10.1016/j.oregeorev.2021.104440

Ohta, J., Yasukawa, K., Nozaki, T., Takaya, Y., Mimura, K., Fujinaga, K., et al. (2020). Fish proliferation and rare-earth deposition by topographically induced upwelling at the late Eocene cooling event. *Scientific Reports*, *10*(1), 9896. https://doi.org/10.1038/s41598-020-66835-8

Pattan, J. N., Pearce, N. J. G., & Mislankar, P. G. (2005). Constraints in using Cerium-anomaly of bulk sediments as an indicator of paleo bottom water redox environment: A case study from the Central Indian Ocean Basin. *Chemical Geology*, *221*(3–4), 260–278. https://doi.org/10.1016/j.chemgeo.2005.06.009

Paul, S. A. L., Volz, J. B., Bau, M., Köster, M., Kasten, S., & Koschinsky, A. (2019). Calcium phosphate control of REY patterns of siliceous-ooze-rich deep-sea sediments from the central equatorial Pacific. *Geochimica et Cosmochimica Acta*, *251*, 56–72. https://doi.org/10.1016/j.gca.2019.02.019

Pavlova, L. M., Shumilova, L. P., Radomskaya, V. I., Ivanov, V. V., Noskova, L. P., & Leusova, N. Y. (2023). Sorption of rare Earth elements by organic matter from aqueous solutions according to experimental data. *Doklady Earth Sciences*, *512*(2), 946–952. https://doi.org/10.1134/s1028334x23601207

Pike, C. R., Roberts, A. P., & Verosub, K. L. (1999). Characterizing interactions in fine magnetic particle systems using first order reversal curves. *Journal of Applied Physics*, *85*(9), 6660–6667. https://doi.org/10.1063/1.370176

Piper, D. Z. (1974). Rare earth elements in ferromanganese nodules and other marine phases. *Geochimica et Cosmochimica Acta*, *38*(7), 1007–1022. https://doi.org/10.1016/0016-7037(74)90002-7

Ren, J., He, G., Yang, Y., Yu, M., Deng, Y., Pang, Y., et al. (2024). Ultraselective enrichment of trace elements in seawater by Co-rich ferromanganese nodules. *Global and Planetary Change*, *239*, 104498. https://doi.org/10.1016/j.gloplacha.2024.104498

Ren, J., Liu, Y., Wang, F., He, G., Deng, X., Wei, Z., & Yao, H. (2021). Mechanism and influencing factors of REY enrichment in deep-sea sediments. *Minerals*, *11*(2), 196. https://doi.org/10.3390/min11020196

Resing, J. A., Sedwick, P. N., German, C. R., Jenkins, W. J., Moffett, J. W., Sohst, B. M., & Tagliabue, A. (2015). Basin-scale transport of hydrothermal dissolved metals across the South Pacific Ocean. *Nature*, *523*(7559), 200–203. https://doi.org/10.1038/nature14577

Roberts, A. P. (2015). Magnetic mineral diagenesis. *Earth-Science Reviews*, *151*, 1–47. https://doi.org/10.1016/j.earscirev.2015.09.010

Roberts, A. P., Chang, L., Heslop, D., Florindo, F., & Larrasoaña, J. C. (2012). Searching for single domain magnetite in the "pseudo-single-domain" sedimentary haystack: Implications of biogenic magnetite preservation for sediment magnetism and relative paleointensity determinations. *Journal of Geophysical Research*, *117*(B8). https://doi.org/10.1029/2012jb009412

Roberts, A. P., Florindo, F., Villa, G., Chang, L., Jovane, L., Bohaty, S. M., et al. (2011). Magnetotactic bacterial abundance in pelagic marine environments is limited by organic carbon flux and availability of dissolved iron. *Earth and Planetary Science Letters*, *310*(3–4), 441–452. https://doi.org/10.1016/j.epsl.2011.08.011

Roberts, A. P., Pike, C. R., & Verosub, K. L. (2000). First-order reversal curve diagrams: A new tool for characterizing the magnetic properties of natural samples. *Journal of Geophysical Research*, *105*(B12), 28461–28475. https://doi.org/10.1029/2000jb900326

Schine, C. M. S., Alderkamp, A.-C., Van Dijken, G., Gerringa, L. J. A., Sergi, S., Laan, P., et al. (2021). Massive Southern Ocean phytoplankton bloom fed by iron of possible hydrothermal origin. *Nature Communications*, *12*(1), 1211. https://doi.org/10.1038/s41467-021-21339-5

Schoepfer, S. D., Shen, J., Wei, H., Tyson, R. V., Ingall, E., & Algeo, T. J. (2015). Total organic carbon, organic phosphorus, and biogenic barium fluxes as proxies for paleomarine productivity. *Earth-Science Reviews*, *149*, 23–52. https://doi.org/10.1016/j.earscirev.2014.08.017

Shi, X., Bi, D., Huang, M., Yu, M., Luo, Y., Zhou, T., et al. (2021). Distribution and metallogenesis of deep-sea rare earth elements. *Geological Bulletin of China*, *40*, 195–208.

Shi, X., Fu, Y., Li, B., Huang, M., Ren, X., Liu, J., et al. (2021). Research on deep-sea minerals in China: Progress and discovery (2011-2020). *Bulletin of Mineralogy, Petrology and Geochemistry*, *40*(2), 305–318.

Tagliabue, A., Bopp, L., Dutay, J.-C., Bowie, A. R., Chever, F., Jean-Baptiste, P., et al. (2010). Hydrothermal contribution to the oceanic dissolved iron inventory. *Nature Geoscience*, *3*(4), 252–256. https://doi.org/10.1038/ngeo818

Takahashi, Y., Hayasaka, Y., Morita, K., Kashiwabara, T., Nakada, R., Marcus, M. A., et al. (2015). Transfer of rare earth elements (REE) from manganese oxides to phosphates during early diagenesis in pelagic sediments inferred from REE patterns, X-ray absorption spectroscopy, and chemical leaching method. *Geochemical Journal*, *49*(6), 653–674. https://doi.org/10.2343/geochemj.2.0393

Takaya, Y., Yasukawa, K., Kawasaki, T., Fujinaga, K., Ohta, J., Usui, Y., et al. (2018). The tremendous potential of deep-sea mud as a source of rare-earth elements. *Scientific Reports*, *8*(1), 5763. https://doi.org/10.1038/s41598-018-23948-5

Tostevin, R., Shields, G. A., Tarbuck, G. M., He, T., Clarkson, M. O., & Wood, R. A. (2016). Effective use of cerium anomalies as a redox proxy in carbonate-dominated marine settings. *Chemical Geology*, *438*, 146–162. https://doi.org/10.1016/j.chemgeo.2016.06.027

Wang, F., He, G., Deng, X., Yang, Y., & Ren, J. (2021). Fish teeth Sr isotope stratigraphy and Nd isotope variations: New insights on REY enrichments in deep-sea sediments in the Pacific. *Journal of Marine Science and Engineering*, *9*(12), 1379. https://doi.org/10.3390/jmse9121379

Wang, Y. L., Liu, Y.-G., & Schmitt, R. A. (1986). Rare earth element geochemistry of South Atlantic deep sea sediments: Ce anomaly change at ~54 My. *Geochimica et Cosmochimica Acta*, *50*(7), 1337–1355. https://doi.org/10.1016/0016-7037(86)90310-8

Yamazaki, T. (2012). Paleoposition of the Intertropical Convergence Zone in the eastern Pacific inferred from glacial-interglacial changes in terrigenous and biogenic magnetic mineral fractions. *Geology*, *40*(2), 151–154. https://doi.org/10.1130/g32646.1

Yamazaki, T., Fu, W., Shimono, T., & Usui, Y. (2020). Unmixing biogenic and terrigenous magnetic mineral components in red clay of the Pacific Ocean using principal component analyses of first-order reversal curve diagrams and paleoenvironmental implications. *Earth Planets and Space*, *72*(1), 120. https://doi.org/10.1186/s40623-020-01248-5

Yamazaki, T., & Horiuchi, K. (2016). Precessional control on ocean productivity in the Western Pacific Warm Pool for the last 400 kyr: Insight from biogenic magnetite. *Geochemistry, Geophysics, Geosystems*, *17*(11), 4399–4412. https://doi.org/10.1002/2016GC006446

Yamazaki, T., & Ikehara, M. (2012). Origin of magnetic mineral concentration variation in the Southern Ocean. *Paleoceanography*, *27*(2). https://doi.org/10.1029/2011PA002271

Yamazaki, T., Suzuki, Y., Kouduka, M., & Kawamura, N. (2019). Dependence of bacterial magnetosome morphology on chemical conditions in deep-sea sediments. *Earth and Planetary Science Letters*, *513*, 135–143. https://doi.org/10.1016/j.epsl.2019.02.015

Yasukawa, K., Nakamura, K., Fujinaga, K., Iwamori, H., & Kato, Y. (2016). Tracking the spatiotemporal variations of statistically independent components involving enrichment of rare-earth elements in deep-sea sediments. *Scientific Reports*, *6*(1), 29603. https://doi.org/10.1038/srep29603

Zhang, Q., Liu, Q., Roberts, A. P., Yu, J., Liu, Y., & Li, J. (2021). Magnetotactic bacterial activity in the North Pacific Ocean and its relationship to Asian dust inputs and primary productivity since 8.0 Ma. *Geophysical Research Letters*, *48*(15), e2021GL094687. https://doi.org/10.1029/2021GL094687

Zhang, Q., Roberts, A. P., Ge, S., Liu, Y., Liu, J., Liu, S., et al. (2022). Interpretation of anhysteretic remanent magnetization carriers in Magnetofossil-Rich marine sediments. *Journal of Geophysical Research: Solid Earth*, *127*(11), e2022JB024432. https://doi.org/10.1029/2022JB024432

Zhou, T., Shi, X., Huang, M., Yu, M., Bi, D., Ren, X., et al. (2020). The influence of hydrothermal fluids on the REY-rich deep-sea sediments in the Yupanqui Basin, Eastern South Pacific Ocean: Constraints from bulk sediment geochemistry and mineralogical characteristics. *Minerals*, *10*(12), 1141. https://doi.org/10.3390/min10121141